Polarization properties of (1̄100) and (112̄0) SiC surfaces from first principles

Giuseppe Piero Brandino and Giancarlo Cicero
Physics Department, Torino Polytechnic, C. Duca degli Abruzzi, 24, I-10129 Torino, Italy
and CNR-IMEM, I-43100 Parma, Italy

Benedetta Bonferroni, Andrea Ferretti, Arrigo Calzolari, and Carlo Maria Bertoni
CNR-INFM National Center on nanoStructures and bioSystems at Surfaces (S3), Via Campi 213/A, I-41100 Modena, Italy
and Dipartimento di Fisica, Università di Modena e Reggio Emilia, Via Campi 213/A, I-41100 Modena, Italy

Alessandra Catellani
CNR-IMEM, Parco Area delle Scienze, 37A, I-43100 Parma, Italy
and CNR-INFM-S3, Via Campi 213/A, I-41100 Modena, Italy

We report on first-principles density functional calculations of nonpolar low-index surfaces of hexagonal silicon carbide. We provide an accurate analysis of the macroscopic bulk spontaneous polarization as a function of the hexagonality of the compound, and we describe in detail the electronic and structural properties of the relaxed surfaces. We revise the methodology to achieve a detailed description of the surface polarization effects. Our results on low-index surfaces reveal a strong in-plane polar contribution, opposing the spontaneous polarization field present in hexagonal polytypes. This in-plane surface polarization component has not been considered before, although it is of significant impact in adsorption experiments, affecting functionalization and growth processes, as well as the electronic properties of confined, low-dimensional systems.

I. INTRODUCTION

The spontaneous polarization in solids has been intensively investigated, since it is responsible for intrinsic physical properties of matter (e.g., ferroelectricity, pyroelectricity, high-k dielectric behavior, etc.) that may be profitably exploited in technological applications. However, despite its intuitive meaning, the theoretical description from an atomistic point of view is a challenging problem. The spontaneous polarization of a material is experimentally accessible but its direct calculation is impractical.[1] In 1993, Resta[2] and King-Smith and Vanderbilt[3] proposed a theoretical approach based on the evaluation of the Berry phase (BP) or equivalently of the centers of Wannier functions (WFs). On the basis of this approach, the polarization properties (spontaneous polarization, Born charges, piezoelectric tensor, ferroelectric properties, etc) of several bulk materials—such as metal oxides (BeO, and ZnO),[4,5] III-V nitrides (GaN, AlN, and InN),[6] perovskites (BaTiO$_3$, PbTiO$_3$, and KNBO$_3$),[7–11] and ionic compounds (LiF, LiCl, and NaCl)[12]—have been routinely calculated.

Despite the wide investigation of bulk system properties, very few reports are dedicated to surfaces[13–15] or low-dimensional cases.[16] Polarization effects may highly influence the characteristics of surfaces, being responsible for surface relaxation and affecting the interaction with adatoms and molecules,[17,18] and consequently of impact on the functionalization and growth processes. Moreover, they are also relevant for thin film technology, since the polarization behavior of a few layers of material may largely differ from the bulk ones.

It is a common custom to refer to the surfaces for which the projection of the spontaneous bulk polarization vector along the normal to the surface is zero as *nonpolar* ones. However, further electrostatic effects may arise at the surface due to the presence of dangling bonds. The rearrangement of the bonding at surfaces leads to a charge displacement that may deeply modify the polarization properties of the surface with respect to the bulk.[19,20]

In this paper, we investigate the polarization properties of a class of *nonpolar* semiconductor surfaces, along directions both parallel and perpendicular to the surface. In particular, we focus on the polarity effects induced by the surface formation with quantitative comparison to the bulk spontaneous polarization. In this frame, we highlight benefits and limits of the different techniques and propose a methodology to evaluate the local dipole moment. We selected silicon carbide as a prototype material to study bulk and surface spontaneous polarization because of the different polytypes existing in nature,[21–23] which exhibit different polarization properties. Polytypes only differ for the stacking sequence of the basic tetrahedral units and are characterized by a partial charge transfer (from silicon to carbon atoms) imparting some ionicity to the bond.[24] Amongst the various polytypes, the most common and studied are the cubic and the hexagonal ones, which can be further distinguished by the number of bilayers representing the minimum repeating unit along the stacking direction.[25–27] Both the zinc-blende and hexagonal systems are noncentrosymmetric and can thus sustain the piezoelectric effect; furthermore, the hexagonal structures exhibit a unique rotation axis (the polar sixfold axis) and are thus compatible with the conditions for pyroelectricity.[19]

First, we evaluated the bulk spontaneous polarization of selected SiC polytypes of decreasing *hexagonality* (2*H*, 4*H*, and 6*H*, the latter one being closer to the cubic system)[21–23] by using two different numerical implementations based on

both the BP and WFs. This allowed us to test the method, comparing our results with previously reported values,[28,29] and to obtain surface and bulk quantities with comparable computational accuracy. Then, we studied the (1×1) relaxed $(1\bar{1}00)$ and $(11\bar{2}0)$ surfaces of $2H$-SiC. We analyzed the structural and electronic properties of these surfaces as well as their polarization behaviors using the WF approach. The formation of buckled Si-C bonds associated with the creation of the surface is responsible for a net dipole along the direction normal to the surface. More remarkably, we observed a large change in the in-plane component of polarization, opposing the bulk spontaneous polarization. This variation is consistent with the direction of the local electric field along the surface Si-C bond.

The evaluation of the in-plane contribution, usually neglected in standard calculations, constitutes one of the most relevant achievements of the present work; indeed, the strong change in polarization at the surface can dramatically affect the interaction of a material with the environment and, in particular, it may be of significant impact in adsorption experiments.[18] For example, in the case of noncovalent functionalization of surfaces with organic molecules, the components of the dipoles both parallel and perpendicular to the surface influence the packing and the geometry of the self-assembly. Growth processes performed employing polar molecules (precursors) will as well interact with surface dipoles.

The paper is organized as follows: Section II describes the theoretical basis of the method as well as the computational details adopted in this work. The main results for the SiC polytypes and surfaces are presented in Secs. III A and III B, respectively; conclusions are reported in Sec. IV.

II. METHOD

A. Theory

The complete description of the theoretical method to address the spontaneous polarization has been extensively reported elsewhere;[2,3] here, we briefly describe the most relevant features of the scheme employed in this work.

The spontaneous polarization $\Delta \mathbf{P}$ of a bulk system has been evaluated as the difference between the structure in study and a reference structure, having null polarization by symmetry.[19,20] One of the prerequisites of this approach is that the two structures have to be connected by an adiabatic transformation, described by a parameter (λ), during which the system must remain an insulator. $\Delta \mathbf{P}$ can be decomposed into an ionic and an electronic component as $\Delta \mathbf{P} = \Delta \mathbf{P}_{ion} + \Delta \mathbf{P}_{el}$. Labeling (0) and (1) the reference and the final configurations over the adiabatic transformation (λ), the ionic component is trivially given by

$$\Delta \mathbf{P}_{ion} = \frac{+e}{\Omega} \sum_I Z_I (\boldsymbol{\tau}_I^{(1)} - \boldsymbol{\tau}_I^{(0)}), \qquad (1)$$

where e is the electron charge and Ω is the cell volume; the summation over I runs over the ionic sites $\boldsymbol{\tau}_I^{(\lambda)}$ and Z_I is the valence charge of the Ith atom.

The electronic component $\Delta \mathbf{P}_{el}$ may be evaluated in terms of the variation of the BP of the electronic Bloch functions along the transformation (λ):

$$\mathbf{P}_{el}^{(\lambda)} = -\frac{2ei}{(2\pi)^3} \sum_n \int_{BZ} d^3\mathbf{k} \langle u_{\mathbf{k}n}^{(\lambda)} | \nabla_{\mathbf{k}} | u_{\mathbf{k}n}^{(\lambda)} \rangle, \qquad (2)$$

where $u_{\mathbf{k}n}$ is the periodic part of the double occupied Bloch states and the sum over n is taken on occupied bands.[30]

Following the formulation provided by Blount,[31] we write the expectation value of the position operator $\hat{\mathbf{r}}$ on the WF $\{|w_n^{(\lambda)}\rangle\}$ basis set as

$$\langle \hat{\mathbf{r}} \rangle_n^{(\lambda)} = \langle w_n^{(\lambda)} | \hat{\mathbf{r}} | w_n^{(\lambda)} \rangle = i \frac{\Omega}{(2\pi)^3} \int_{BZ} d^3\mathbf{k} \langle u_{\mathbf{k}n}^{(\lambda)} | \nabla_{\mathbf{k}} | u_{\mathbf{k}n}^{(\lambda)} \rangle. \quad (3)$$

Thus, Eq. (2) may be expressed in terms of the centers of charge $\langle \hat{\mathbf{r}} \rangle_n^{(\lambda)}$ of the WFs of the occupied bands:

$$\mathbf{P}_{el}^{(\lambda)} = -\frac{2e}{\Omega} \sum_n \langle \hat{\mathbf{r}} \rangle_n^{(\lambda)}. \qquad (4)$$

Despite the formal equivalence of the two implementations (BP and WFs), the Wannier centers provide an intuitive correspondence with the concept of *electron localization* that is used in the classical definition of the macroscopic polarization.[32]

We note that for a bulk system the spontaneous polarization is a multivalued quantity (measured in C/m^2), defined $\text{mod}(\frac{e}{\Omega}\mathbf{R})$, where $\mathbf{R}$ is a vector of the three-dimensional direct lattice. The case of surfaces is different since the quantities of interest are generally defined with respect to the surface unit area. Therefore, to quantify the polarization properties of surfaces, we will adopt the use of an in-plane polarization as the dipole moment per unit area (measured in C/m). We note that while the BP approach can be used to calculate the total polarization for a slab in the supercell approach, where a (fictitious) periodicity is always maintained, whenever the periodicity is broken, the local contribution of the polarization, or the projections along, e.g., interface planes, is in general, ill defined.

In this work, we propose a unified scheme for the calculation of the polarization effects in surfaces and interfaces. We exploit the localization properties of the WF set that allow us to treat the system as an ensemble of classical point charges. Furthermore, noting that the surfaces are periodic in two directions but nonperiodic in the third one, we show how to calculate separately the in-plane (periodic) and perpendicular (nonperiodic) contributions of the polarization. The proposed procedure provides a physical picture which is consistent with the polarization properties of the corresponding bulk. This approach is indeed the natural extension of the method described above for the bulk system: The polarization stems from the neutralization of localized charges associated with the ions and to the WFs included in the simulation supercell.

In the study of surfaces, to assign a surface property, one needs to define a region where significant changes from the bulk occur to the same property in the presence of a surface; this definition is thus associated with a decaying length, as

the distance from surface, where this deviation is observable. In particular, in order to analyze the polarization effect, while moving from the bulk toward the surface, it is useful to define a minimal volume in such a way that the local (in plane, or two dimensional) polarization can be defined on the same ground of the bulk.

In a recent paper, Wu *et al.*[33] proposed a definition of the polarization for an interface structure as the sum of dipoles, calculated in subunits obtained by partitioning the simulation supercell in the direction perpendicular to the layers. In the specific case of perovskite materials, such as $BaTiO_3$ or $SrTiO_3$,[33] the Wannier centers are naturally localized in atomic layers. This allows one to have a layer-by-layer decomposition of the polarization in the slab. In other words, such localization leads to the definition of the in-plane polarization over a building block (one single atomic layer) smaller than the natural unit cell of the corresponding bulk phase (two layers). Although formally correct, this localization method does not allow a direct comparison with bulk values.

As an alternative to a pure WFs approach, we propose a procedure to define the polarization for finite systems in such a way as to reproduce the bulk value in the limit of infinite slab thickness. In order to define the in-plane (periodic) quantities and decouple the bulk and surface contributions to polarization, we make use of the extrapolation scheme originally proposed for the surface energy by Fiorentini and Methfessel.[34] On the other hand, the perpendicular contribution (nonperiodic) to the surface polarization can be described by macroscopically averaging the electrostatic potential (local ionic term+Hartree potential) over suitable intervals in the slab, following the technique proposed by Baldereschi *et al.*[35] The combination of the two approaches allows us to define the minimal cell over which we can evaluate the polarization of the system.

The extrapolation method[34] consists in evaluating the surface polarization for slabs $\mathbf{p}_{slab}$ of increasing thickness. The total supercell polarization is the sum of n bulk units, not yet specified, plus the surface contribution $\mathbf{p}_{surf}$ (or two times $\mathbf{p}_{surf}$ for symmetric slabs):

$$\mathbf{p}_{slab} = 2\mathbf{p}_{surf} + n\mathbf{p}_{bulk}. \quad (5)$$

The fitting from Eq. (5) depends on how many units n constitute the bulk part of the slab, i.e., it depends on how the slab is partitioned on surface and bulk contributions and on the size of each bulk unit. This subdivision alters the reciprocal weight of surface and bulk contributions. The proper setting of the spacer n allows one to recover the value of the bulk spontaneous polarization. The smallest volume that realizes the condition for the fit in Eq. (5) fulfills the request of minimal meaningful unit to compare bulk and surface properties.

The perpendicular contribution of the total surface dipole p_z can also be estimated via the ionization potential (I_p). This quantity is directly accessible to experiments, and it is obtained with respect to the vacuum level of the slab calculation from the macroscopic average of the electrostatic potential.[35,36] The average is performed by integration over a length L, which should be chosen so that $L=nc$, where c is a typical length of the system, related to the bulk periodicity in the z direction. The minimal volume is thus defined when the extrapolation (for the parallel component) and the macroscopic average (for the z component) provide the same slab subdivision in n units. In principle, such a unit may be smaller than the unit cell. This happens every time the periodicity of the macroscopic average of the potential is higher than the periodicity of the underlying lattice.

The polarization effects on the surface should be related to the projection of the bulk polarization vector along the direction normal to the surface. However, the details of our results highlight a more complex scenario: The surface effects may deeply modify the polarization properties of the infinite periodic structure, with no direct correlation to the bulk value.

B. Computational details

We performed *ab initio* density functional theory (DFT) calculations, in the plane wave pseudopotential framework, as implemented in the PWSCF package.[37] We used ultrasoft pseudopotentials[38] and the PBE[39] approximation to the exchange-correlation functional. A kinetic energy cutoff of 30 Ry (300 Ry) for the wave functions (charge density) was found to give converged bulk properties.

Bulk calculations were performed in a C_{3v} supercell (24 atoms) that contains replicas of the full stacking sequence along the z direction to maintain comparable computational accuracy for all the polytypes. The SiC surfaces were instead represented by slabs with two and four atoms per layer for the $(1\bar{1}00)$ and $(11\bar{2}0)$ surfaces, respectively. We checked the effects of the slab thickness by varying the number of layers from 10 to 16 in the case of $(1\bar{1}00)$ and from 8 to 12 in the case of $(11\bar{2}0)$ surface. For both surfaces, a thick space of vacuum (~ 10 Å) is included in the direction perpendicular to the surface in order to avoid spurious interactions among adjacent replicas.

The integration on the Brillouin zone was performed by using a $\mathbf{k}$-point grid of $(10 \times 10 \times 4)$ for bulk calculations and $(6 \times 6 \times 1)$ for $(1\bar{1}00)$ and $(11\bar{2}0)$ surfaces.[40] Both bulk and surface systems were fully relaxed (no fixed atom position) until the forces varied less than 0.03 eV/Å. We note that the spontaneous polarization is a slow converging quantity with respect to Brillouin zone sampling, much more sensitive than standard quantities evaluated in DFT calculations, such as the total energy, the charge density, etc.

We evaluated the polarization using the BP approach included in the PWSCF package[37] as well as the WF approach as implemented in the WANT[41,42] code. We note that no layer-by-layer decomposition is possible when using the BP approach, as mentioned above. The WFs and the corresponding centers [Eq. (3)] are calculated following the *maximum localization* procedure proposed by Marzari and Vanderbilt[43] and successively extended to the ultrasoft pseudopotential case.[44]

Every bulk polarization calculation requires a reference structure, since only changes in polarization are defined. The simplest reference structure when dealing with hexagonal

TABLE I. Computed and experimental structural parameters for different hexagonal (H) and cubic (C) bulk SiC polytypes. The lattice parameters have been optimized using Murnaghan equation of state.

		This work	Theory[a]	Expt.[b]	Expt.[c]
2H	a (Å)	3.096	3.105	3.076	
	c (Å)	5.080	5.113	5.048	
	c/a	1.641	1.647	1.640	
4H	a (Å)	3.094	3.108		3.073
	c (Å)	10.142	10.186		10.053
	c/a	3.278	3.277		3.268
6H	a (Å)	3.094	3.062		3.081
	c (Å)	15.206	15.014		15.117
	$c//a$	4.915	4.903		4.907
3C	a (Å)	4.384	4.402	4.360	

[a]Reference 22.
[b]References 21 and 27.
[c]Reference 45.

compounds is the zinc blende ($3C$) due to the fact that its polarization can be set to zero on the base of symmetry considerations, within a proper choice of the unit cell.[19,20] With such a choice, any value different from zero for $3C$ is due to numerical errors. The numerical details of our calculations give a polarization for $3C$ of the order of 10^{-4} C/m^2 in the C_{3v} hexagonal cell. We therefore define this value as the uncertainty of our bulk calculations. For further comparison with the surface structures, we also evaluated the bulk polarization for the $2H$ and $3C$ polytypes using an orthorhombic supercell (using a **k**-point grid of $6 \times 6 \times 6$), equivalent to the one used for surface calculations. In this case, the accuracy of the results is reduced to 10^{-3} C/m^2. We assume this value as the error bar of surface polarization.

III. RESULTS AND DISCUSSION

A. Bulk SiC polytypes

We studied the variation of the spontaneous polarization as a function of the hexagonality, namely, while passing from the $2H$ (the most *hexagonal*) to the $4H$ and $6H$ polytypes.[21,22,26,27]

For each structure, we relaxed both the lattice parameters and the atomic positions in the cell. The equilibrium data (Table I) show the typical behavior of PBE calculations, with lattice parameters overestimated of roughly 1% with respect to experiment,[21] and in good agreement with previous first-principles calculations.[22]

We evaluated the polarization of the three SiC polytypes using both the BP and the WF approaches. In both cases, the components of the spontaneous polarization result to be zero by symmetry in the plane orthogonal to the stacking direction. The results for the component of the polarization in the stacking direction are summarized in Table II.

TABLE II. Spontaneous polarization along the stacking direction calculated both with BP and WF approaches. Experimental and other theoretical values are also reported for comparison. All the values are expressed in C/m^2. The values for the $3C$ polytypes both in a hexagonal and orthorhombic cell are reported as a reference.

	BP	WFs	Theory[a]	Expt.[b]
2H	−0.046	−0.048	−0.043	
2H[c]		−0.043		
4H	−0.021	−0.023	−0.018	−0.01
6H	−0.015	−0.015	−0.009	
3C	0.0001	0.0001		
3C[d]	0.0010	0.0013		

[a]Reference 28.
[b]Reference 29.
[c]$2H$ in orthorhombic cell with z along a nonpolar direction ($[1\bar{1}00]$ or $[11\bar{2}0]$).
[d]$3C$ in orthorhombic cell.

For all the polytypes, we found similar results using both BF and WF approaches. Both sets of values are in very good agreement with the published theoretical[28] and the experimental[29] results. We also note that the spontaneous polarization decreases linearly from $2H$ to $6H$, as a function of the number of bond inversions along the stacking direction, approaching as a limiting case the $3C$ structure (Fig. 1).

B. Low-index nonpolar SiC surfaces

The main goal of this work is to understand any possible relation between the intrinsic spontaneous polarization and the charge transfer occurring upon surface formation at the so-called nonpolar surfaces. For crystal lattices that present a
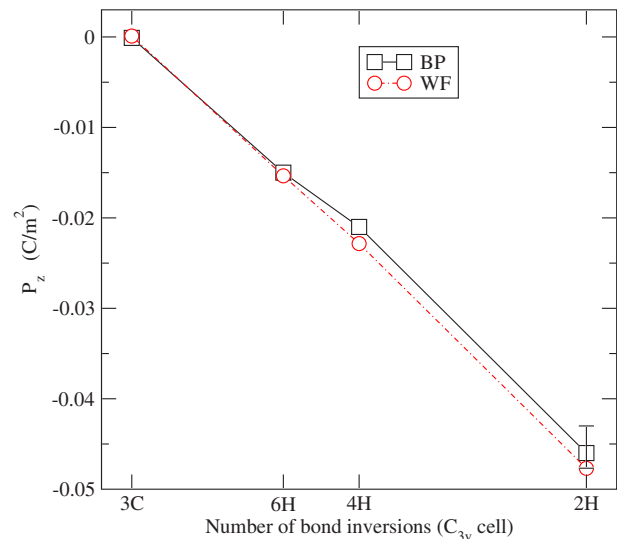

FIG. 1. (Color online) Spontaneous bulk polarization as a function of the number of bond inversions in a C_{3v} cell. The error bar is estimated from the minimum and the maximum values of the polarization calculated on different supercells.
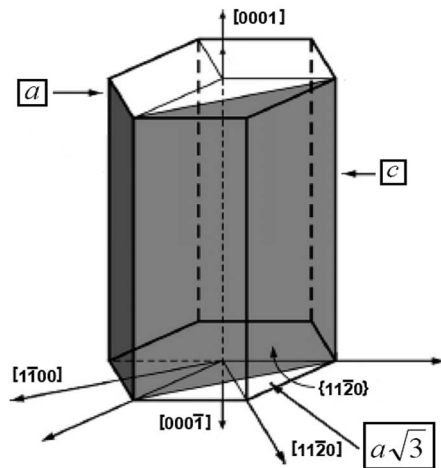
FIG. 2. Hexagonal cell with the polar (0001) and nonpolar (1$\bar{1}$00) and (11$\bar{2}$0) surfaces highlighted in gray.

bulk spontaneous polarization, the term nonpolar surface indicates a plane containing the polarization axis. It is known[19] that surface effects can cancel the spontaneous polarization even at polar surfaces via reconstruction, adatoms, or vacancy formation.[17,40] It is desirable to understand and quantify the polarization close to the surface, in view of the selected applications such as adsorption, ultrathin films, or nanodevices, where surface properties play the major role.

We considered two low-index SiC surfaces, namely, the (1$\bar{1}$00) and (11$\bar{2}$0) surfaces. For these surfaces, the (1×1) periodicity is stable,[40] although different preparation conditions may give rise to reconstructions.[46–48] For the sake of simplicity, we focused on the (1×1) clean relaxed surfaces, thus avoiding possible effects arising from surface reconstruction.

As shown in Fig. 2, both surfaces would be referred to as nonpolar, since they present the stacking direction ([0001], the polar direction in the bulk) parallel to the surface plane. These surfaces constitute the simplest example to address the problem of surface dipole formation, stemming from two decoupled terms, the bulk and the surface, respectively. The study of the polar SiC(0001) surface constitutes a much more complicated case. The surface undergoes a strong reconstruction, which includes the presence of Si adatoms to stabilize the structure.[40] Moreover, both the ideal and the reconstructed (0001) surfaces result to be metallic in DFT calculations,[49] invalidating the goal of the work, which requires an insulating system.

In the following, we will focus on the wurtzite (2H) polytype. Even though 2H is not easily accessible from the experimental point of view (but see Ref. 27), this constitutes a template for developing a general method in evaluating surface polarization effects. The case of the other polytypes would be straightforward, although computationally more demanding.

1. SiC(1$\bar{1}$00) surface

We simulated the SiC(1$\bar{1}$00) surface in a repeated slab geometry. For this surface, two terminations are possible,
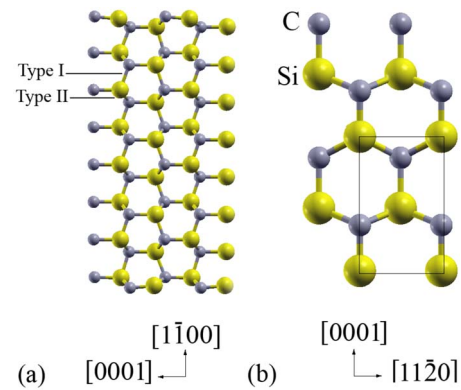

FIG. 3. (Color online) (a) Side and (b) top views of the relaxed (1$\bar{1}$00) surface (Ref. 50). The hexagonal stacking direction is the [0001] direction. The larger spheres (yellow) indicate silicon atoms, while the smaller ones (gray) stand for carbon atoms. The possible terminations are indicated as type I and type II. The rectangular zone sketched in (b) identifies the surface unit cell used in the simulations.

usually labeled type I and type II (shuffle and glide planes respectively), as displayed in Fig. 3. The analysis of the two terminations shows that type II truncation gives rise to a metallic surface, which is energetically less favorable than type I. For these reasons we focus on type I surfaces.

The polar [0001] axis lies along the y direction [Fig. 3(b)], while the z axis is perpendicular to the surface. In order to reduce rounding errors, we chose the most symmetric slab; this leads to an even number of layers. While we found that a 12-layer slab gives converged structural and electronic properties, a 16-layer slab is required to get converged surface polarization values. Results for the 16-layer slab are shown in Table III.

The surface relaxation mainly involves the outer Si and C layers. The Si-C surface bonds are tilted by ~5.2°, with the silicon atom relaxing inward by 0.26 Å. These findings are in good agreement with previous results.[51] The surface energies are calculated using the linear extrapolation approach at increasing slab thickness.[34] We obtained a value of

TABLE III. Details of the relaxed nonpolar (1$\bar{1}$00) surface in comparison with published data: tilt angle ω of the surface bond, bond length BL (in Å and % of the corresponding bulk value) of the surface bonds, surface energy per surface unit area σ, displacements along the perpendicular direction for surface atoms ($d_{\perp Si}$ and $d_{\perp C}$) and ionization potential I_p.

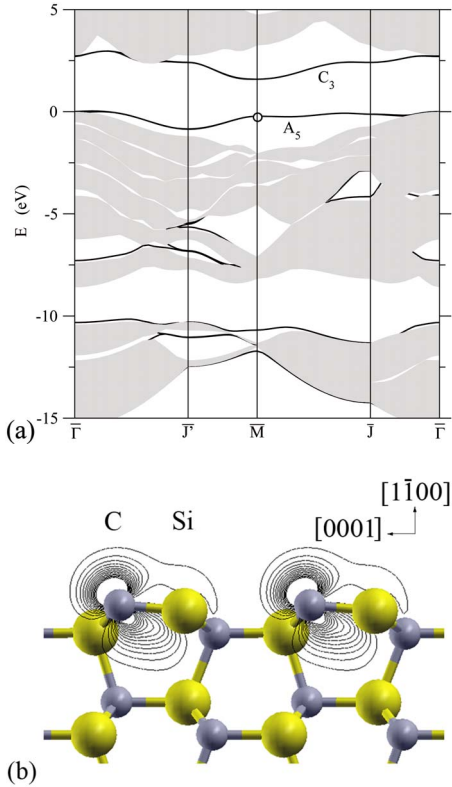|	This work	LDA[a]	SCC-DFTB[b]
ω (deg)	5.2	3.8	2.4
BL (Å)	1.74 (−8.9)	1.71 (−9.0%)	1.73 (−8.2%)
$d_{\perp Si}$ (Å)	−0.26	−0.28	−0.02
$d_{\perp C}$ (Å)	−0.10	−0.17	−0.01
σ (eV/Å^2)	0.15		0.19
I_p (eV)	5.60		

[a]Reference 51.
[b]Reference 48.

FIG. 4. (Color online) (a) Surface band structure of the relaxed SiC ($1\bar{1}00$) surface. The shaded area indicates the projected bulk band structure, and continuous lines indicate surface states. The zero of the energy scale is taken as the bulk valence band top. (b) Isocontour plot of the HOMO surface state calculated in $\bar{M}$, identified as a circle in panel (a).

0.15 eV/Å^2, in agreement with other theoretical results obtained for similar SiC surfaces.[48,52]

The surface projected bulk band structure is shown in Fig. 4(a); continuous lines identify the surface states. Two surface states in the band gap are present, one occupied and the other empty, in agreement with, e.g., Ref. 51. The isocontour plot for the highest occupied molecular orbital (HOMO) [Fig. 4(b)] shows that the charge density is mainly localized on the surface Si-C bond, with charge transfer from Si to C, which strengthens the surface bond. This behavior is consistent with the observed relaxation mechanism where the "depleted" Si moves inside the surface, leaving C as the outermost atom.[40,51]

To understand the surface effect on the polarization behavior while moving from the surface to bulk, we need to define the minimal unit on which the surface polarization can be calculated. From Fig. 3, we see that the periodic units for this slab are formed of four layers. The application of the procedure proposed in Sec. II A yields a different result. Indeed, two layers are already sufficient to reproduce the polarization of the bulk system. Such a cell constitutes the minimal unit over which we will evaluate the surface polarization.

A unit-by-unit analysis shows that after four layers, the surface polarization converges to the bulk values, as shown
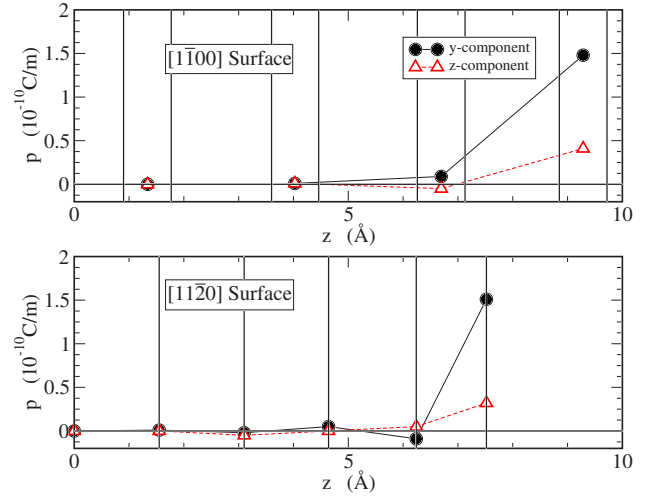

FIG. 5. (Color online) Unit-by-unit difference of the surface polarization with respect to the bulk value for ($1\bar{1}00$) and ($11\bar{2}0$) surfaces (C/m). The zero is set in the center of the slab. Circles indicate the y component, parallel to the surface and to the stacking direction. Triangles indicate the z component, perpendicular to the surface. Vertical lines indicate the position of the atomic layers.

in Fig. 5. Here, we see that the creation of a surface strongly modifies the polarization. Adding up all the contributions of the different units, we evaluate the surface effect as the deviation from the bulk value; the results are summarized in Table IV. The component of the surface polarization normal to the surface (the positive direction is oriented outward) is $p_z = 0.35 \times 10^{-10}$ C/m, to be compared to a bulk term which is zero.

The large charge transfer that occurs along the surface bond is responsible also for a large in-plane dipole component. Analyzing the position of the Wannier centers on the surface, we notice that they are no longer in the tetrahedral configuration typical of the bulk structure; indeed, two of them lie along the surface Si-C bonds, with a total displacement from the bulk position of roughly ~ 0.7 Å. Since each Wannier center carries a $-2e$ electric charge, this corresponds to a contribution to the surface polarization y component equal to $\sim 1.4 \times 10^{-10}$ C/m, to be compared with the bulk spontaneous polarization (-0.12×10^{-10} C/m). The main contribution to surface polarization along the stacking direction (y) comes from the first unit (1.48×10^{-10} C/m), while the units beneath contribute with smaller amounts; their electrons are localized along the Si-C bonds although in a

TABLE IV. Surface polarization for the ($1\bar{1}00$) and ($11\bar{2}0$) surfaces; numerical values are given with respect to the corresponding bulk values. The y direction is parallel to the stacking, which is the direction of bulk spontaneous polarization, and z is perpendicular to the surface. Values are expressed in units of 10^{-10} C/m.

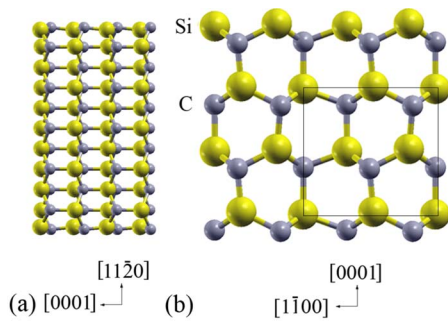|	Δp_x	Δp_y	Δp_z
($1\bar{1}00$) surface	0.00	1.59	0.35
($11\bar{2}0$) surface	0.00	1.45	0.32

FIG. 6. (Color online) (a) Side and top (b) views of the relaxed (11$\bar{2}$0) surface. The hexagonal stacking direction is the [0001] direction. The rectangular zone sketched in (b) identifies the surface unit cell used in the simulations. In the picture, a (2×2) replica of the unit cell is shown. Color code as in Fig. 3.

TABLE V. Structural properties of the relaxed nonpolar (11$\bar{2}$0) surface versus published data: tilt angle ω of the surface bond, bond length BL (in Å and % of the corresponding bulk value) of the surface bonds, surface energy per surface unit area σ, displacements along the perpendicular direction for surface atoms ($d_{\perp_{Si}}$ and $d_{\perp_C}$), and ionization potential I_p.

	This work	SCC-DFT[a]
ω (deg)	5.9	5
BL (Å)	1.76 (−7.9%)	1.76 (−6.7%)
$d_{\perp_{Si}}$ (Å)	−0.22	−0.15
$d_{\perp_C}$ (Å)	−0.04	0.02
σ (eV/Å^2)	0.16	0.20
I_p (eV)	5.65	

[a]Reference 48.

slightly distorted tetrahedral coordination. The x component remains zero as in the bulk. Table IV shows the total excess of the surface polarization with respect to the bulk value, i.e., the sum of the contributions of each unit, as previously discussed. This in-plane component along the stacking direction results to be the strongest contribution to the surface dipole, being about one order of magnitude larger than the spontaneous polarization; furthermore, it contributes with opposite sign, thus it tends to cancel the bulk contribution.

The surface effects on polarization strongly depend on the difference in electronegativity between silicon and carbon atoms, i.e., on the ionicity of the bond, which is responsible for the displacement of WF centers. Large ionicity does not allow electrons to move much from bulk positions, while a smaller one allows bigger displacements. Similar ongoing studies on ZnO surfaces[53] indeed show that surface polarization contributions are lower than those for SiC.

2. SiC(11$\bar{2}$0) surface

In the case of the (11$\bar{2}$0) surface, the two surfaces of the slab are equivalent for any choice of the number of layers, as shown in Fig. 6(a). Here, nine SiC layers are sufficient to reach the convergence in structural parameters. However, to obtain converged surface polarization values, we increased the thickness of the slab up to 12 layers. The unit cell in this surface contains two Si-C bonds, as shown in Fig. 6(b). The structural characteristics of the relaxed surface are reported in Table V.

As for the (1$\bar{1}$00) surface, the relaxation mainly involves the outermost layers, with the outermost Si-C bonds tilted by 5.9° and contracted by −7.9%.

The band structure in Fig. 7 shows the presence of four states, two fully occupied and two empty, 2×2 almost degenerate in energy, localized on the surface. This is related to the presence of the two surface Si-C bonds, with two surface states each. Similar to what happens at the (1$\bar{1}$00) surface, these states correspond to large charge transfer along the surface bonds. In this case, one layer is enough to correctly describe the polarization properties of the system.

Since both the geometrical and electronic properties of the Si-C bonds are close to those of the (1$\bar{1}$00) surface, it would be reasonable to expect also similar results for the surface polarization. Indeed, a layer-by-layer analysis (Fig. 5) reveals that it is possible to recover the bulklike configuration after only four layers. At the outermost layer, we observe the rise of a surface polarization component perpendicular to the surface as well as a large modification of the [0001] component, 1.51×10^{-10} C/m (see Fig. 5). Table IV reports the total excess of the surface polarization with respect to the bulk value, i.e., the sum of the contributions of each layer shown in Fig. 5.

The (11$\bar{2}$0) surface shows a smaller surface polarization with respect to (1$\bar{1}$00), which may be ascribed to a smaller charge transfer, due to different surface truncation. This is consistent also with the smaller bond contraction of the surface Si-C bonds; a smaller amount of charge along the bond results in a weaker, and so longer, bond.

As a consistency check, we apply the extrapolation technique of Sec. II A to evaluate the in-plane component of the dipole moment via BP calculations of the total polarization in
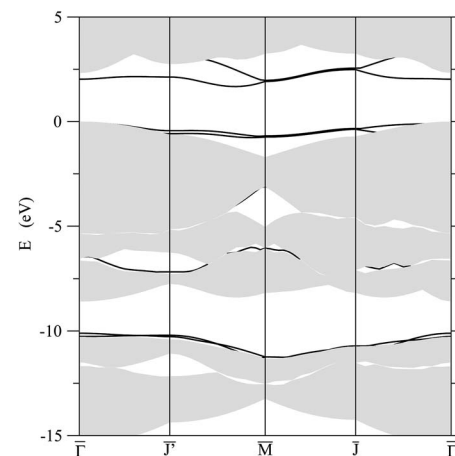

FIG. 7. Surface band structure of the relaxed (11$\bar{2}$0) surface. The shaded area shows the projected bulk band structure, and the solid lines are the surface states.

slabs with different thicknesses; the results are in perfect agreement with the previous data, giving a y dipole component of 1.45×10^{-10} C/m. Furthermore, the component of the local dipole perpendicular to the surface as estimated by means of the ionization potential technique (see Sec. II A) gives $p_z = 0.50 \times 10^{-10}$ C/m, for both surfaces, slightly larger than the WF result.

IV. CONCLUSIONS

In this paper, we have calculated the polarization field in different SiC structures (bulk and surfaces) by means of different approaches. We first studied the bulk spontaneous polarization, to provide a trend as a function of the hexagonality of the structure, for comparison with surfaces. Our results, obtained by means of both BP and WFs, indicate that polarization effects are highly sensitive to the details of the calculation; accurate results can be achieved by improving the **k**-point sampling beyond that typically exploited for structural and electronic investigations.

We proposed a unified scheme to calculate the surface polarization based on the evaluation of the WFs and the average potential profiles; the choice of a proper reference volume over which calculating the in-plane and perpendicular components of the polarization leads to a physical picture that is consistent with the bulk polarization properties of the material. The internal consistency of the proposed method is not fortuitous. Keeping in mind that the spontaneous polarization is a macroscopic property of matter, on one hand, the introduction of WF centers allows us to reduce the problem of a semi-infinite surface to a finite and neutral system of localized charges. On the other hand, the average procedure moves from the atomistic details of the crystalline structure giving a macroscopic picture of the system.

In the case of SiC $(11\bar{2}0)$ and $(1\bar{1}00)$ nonpolar surfaces, we demonstrated that the charge transfer that arises upon truncation of a bulk structure is strong enough to create a large surface polarization along the direction normal to the surface and to deeply modify the surface polarization component along the bulk polar direction for the first film layers. We therefore showed that the commonly called nonpolar surfaces may present remarkable polarity effects. On the other hand, the surface polarization can be considered as a local contribution in thicker slabs, since it approaches the bulk values inside the slabs, within a few atomic layers from the surface.

Finally, we remark that the presence of nonvanishing in-plane polarization components in the case of nonpolar surfaces is fundamental for the understanding of adsorption and interaction mechanisms of adatoms and small molecules at surfaces and to eventually rationalize interface formation. The decaying behavior of the in-plane surface polarization components, which counterbalances and even cancels the one derived from the spontaneous polarization field, poses a question on the size extension of polarization and pyroelectric effects, which may be relevant for nanodevices.

ACKNOWLEDGMENTS

[1] M. Posternak, A. Baldereschi, A. Catellani, and R. Resta, Phys. Rev. Lett. **64**, 1777 (1990).

[2] R. Resta, Rev. Mod. Phys. **66**, 899 (1994).

[3] R. D. King-Smith and D. Vanderbilt, Phys. Rev. B **47**, 1651 (1993).

[4] Y. Noel, C. M. Zicovich-Wilson, B. Civalleri, P. D'Arco, and R. Dovesi, Phys. Rev. B **65**, 014111 (2001).

[5] F. Bernardini and V. Fiorentini, Phys. Rev. B **58**, 15292 (1998).

[6] F. Bernardini, V. Fiorentini, and D. Vanderbilt, Phys. Rev. B **56**, R10024 (1997).

[7] A. Dal Corso, M. Posternak, R. Resta, and A. Baldereschi, Phys. Rev. B **50**, 10715 (1994).

[8] L. Fu, E. Yaschenko, L. Resca, and R. Resta, Phys. Rev. B **60**, 2697 (1999).

[9] S. Dall'Olio, R. Dovesi, and R. Resta, Phys. Rev. B **56**, 10105 (1997).

[10] J. Iniguez, D. Vanderbilt, and L. Bellaiche, Phys. Rev. B **67**, 224107 (2003).

[11] G. Sághi-Szabó, R. E. Cohen, and H. Krakauer, Phys. Rev. B **59**, 12771 (1999).

[12] A. Shukla, Phys. Rev. B **61**, 13277 (2000).

[13] D. Vanderbilt and R. D. King-Smith, Phys. Rev. B **48**, 4442 (1993).

[14] J. Padilla and D. Vanderbilt, Phys. Rev. B **56**, 1625 (1997).

[15] B. Meyer and D. Vanderbilt, Phys. Rev. B **63**, 205426 (2001).

[16] S. M. Nakhmanson, A. Calzolari, V. Meunier, J. Bernholc, and M. B. Nardelli, Phys. Rev. B **67**, 235406 (2003).

[17] C. Noguera, J. Phys.: Condens. Matter **12**, R367 (2000).

[18] J. Zúniga-Pérez, V. Munoz-Sanjosé, E. Palacios-Lidon, and J. Colchero, Phys. Rev. Lett. **95**, 226105 (2005).

[19] J. Nye, *Physical Properties of Crystals* (Oxford University Press, London, 1957).

[20] R. M. Martin, Phys. Rev. B **9**, 1998 (1974).

[21] *Semiconductors: Physics of group IV elements and III-V compounds*, edited by O. Madelung, M. Schultz, and H. Weiss, Landolt-Börnstein, New Series, Group III, Vol. 17, Pt. A (Springer-Verlag, Berlin, 1982).

[22] M. C. Righi, C. A. Pignedoli, G. Borghi, R. Di Felice, C. M. Bertoni, and A. Catellani, Phys. Rev. B **66**, 045320 (2002).

[23] P. Käckell, J. Furthmüller, and F. Bechstedt, Phys. Rev. B **60**, 13261 (1999).

[24] M. Sabisch, P. Kruger, and J. Pollmann, Phys. Rev. B **51**, 13367 (1995).

[25] C. Cheng, R. Needs, and V. Heine, J. Phys. C **21**, 1049 (1988).

[26] F. Bechstedt, P. Käckell, A. Zywietz, K. Karch, B. Adolph, K. Tenelsen, and J. Furthmüller, Phys. Status Solidi B **202**, 35 (1997).

[27] T. L. Daulton, T. J. Bernatowicz, R. S. Lewis, S. Messenger, F. J. Stadermann, and S. Amari, Science **296**, 1852 (2002).

[28] A. Qteish, V. Heine, and R. J. Needs, Phys. Rev. B **45**, 6534 (1992).

[29] S. Bai, R. P. Devaty, W. J. Choyke, U. Kaiser, G. Wagner, and M. F. MacMillan, Appl. Phys. Lett. **83**, 3171 (2003).

[30] The Berry's phase (mod 2π) is defined as $\phi^{(\lambda)}(\mathbf{k},\mathbf{k}') = \text{Im}\{\ln[\det S^{(\lambda)}(\mathbf{k},\mathbf{k}')]\}$, where $S_{mn}^{(\lambda)}(\mathbf{k},\mathbf{k}') = \langle u_{\mathbf{k}m}^{(\lambda)} | u_{\mathbf{k}'n}^{(\lambda)} \rangle$ is the overlap matrix of lattice periodic Bloch function $u^{(\lambda)}$.

[31] E. Blount, Solid State Phys. **13**, 305 (1962).

[32] L. Landau and E. Lifshitz, *Electrodynamics of Continuous Media* (Pergamon, Oxford, 1984).

[33] X. Wu, O. Dieguez, K. M. Rabe, and D. Vanderbilt, Phys. Rev. Lett. **97**, 107602 (2006).

[34] V. Fiorentini and M. Methfessel, J. Phys.: Condens. Matter **8**, 6525 (1996).

[35] A. Baldereschi, S. Baroni, and R. Resta, Phys. Rev. Lett. **61**, 734 (1988).

[36] C. Sgiarovello, N. Binggeli, and A. Baldereschi, Phys. Rev. B **64**, 195305 (2001).

[37] S. Baroni, A. Dal Corso, S. de Gironcoli, and P. Giannozzi, PWSCF package, http://www.pwscf.org

[38] D. Vanderbilt, Phys. Rev. B **41**, 7892 (1990).

[39] J. P. Perdew, K. Burke, and M. Ernzerhof, Phys. Rev. Lett. **77**, 3865 (1996).

[40] M. C. Righi, C. A. Pignedoli, R. Di Felice, C. M. Bertoni, and A. Catellani, Phys. Rev. Lett. **91**, 136101 (2003).

[41] A. Ferretti, B. Bonferroni, A. Calzolari, and M. Buongiorno Nardelli, WANT code, http://www.wannier-transport.org, see also Ref. 42.

[42] A. Calzolari, N. Marzari, I. Souza, and M. B. Nardelli, Phys. Rev. B **69**, 035108 (2004).

[43] N. Marzari and D. Vanderbilt, Phys. Rev. B **56**, 12847 (1997).

[44] A. Ferretti, A. Calzolari, B. Bonferroni, and R. Di Felice, J. Phys.: Condens. Matter **19**, 036215 (2007).

[45] A. Bauer, J. Kräusslich, L. Dressler, P. Kuschnerus, J. Wolf, K. Goetz, P. Käckell, J. Furthmüller, and F. Bechstedt, Phys. Rev. B **57**, 2647 (1998), and references therein.

[46] T. Seyller, R. Graupner, N. Sieber, K. V. Emtsev, L. Ley, A. Tadich, J. D. Riley, and R. C. G. Leckey, Phys. Rev. B **71**, 245333 (2005).

[47] C. Virojanadara and L. I. Johansson, Phys. Rev. B **68**, 125314 (2003).

[48] E. Rauls, J. Elsner, R. Gutierrez, and T. Frauenheim, Solid State Commun. **111**, 459 (1999).

[49] J. E. Northrup and J. Neugebauer, Phys. Rev. B **57**, R4230 (1998).

[50] Figures of crystal structures were created using XCRYSDEN visualization code, http://www.xcrysden.org/; see also A. Kokalj, Comput. Mater. Sci. **28**, 155 (2003).

[51] J. Pollmann, P. Kruger, and M. Sabisch, Phys. Status Solidi B **202**, 421 (1997).

[52] A. Catellani, G. Cicero, and G. Galli, J. Chem. Phys. **124**, 024707 (2006).

[53] G. P. Brandino, G. Cicero, and A. Catellani (unpublished).